Proceeding of the IEEE
International Conference on Robotics and Biomimetics
Dali, China, December 2019

Realization of Complex Terrain and Disturbance Adaptation for Hydraulic Quadruped Robot under Flying trot Gait

Teng Chen[1], Yibin Li[1], Xuewen Rong[1], and Lelai Zhou[1]

Abstract— **To improve the dynamic motion capability of the bionic quadruped robot, a kind of flying trot gait control method is proposed. Planning the motion of the torso and mapping it to the foot, the robot can achieve a stable flying trot movement. The motion controller is designed based on the spring loaded inverted pendulum (SLIP) model to achieve self-recovery stability under the external force disturbance of the robot. The proposed method can achieve the transition between the trot and the flying trot gait, where the flying trot gait can improve the speed of the quadruped robot and trot gait motion has a better robust ability. The dynamic simulation results of Webots verify that the method can achieve three-dimensional stable and robust flying trot gait. The quadruped robot can effectively climb the slopes within 20° in flying trot gait and resist lateral impact forces. Experiments on the physical platform SCalf-III verify the effectiveness of the proposed method to achieve stable flying trot gait.**

I. INTRODUCTION

The dynamic motion of quadruped robots is hard to achieve due to various constraints, such as the construction of non-linear dynamic model, under-actuation of joints, saturation of actuator output torque, and so on. In recent years, great progress has been made in the study of the dynamic gait of quadruped robots. However these studies mainly focus on the trot and walk gaits [1], [2], [3], and these gaits have supporting legs at each moment to keep the balance. Few robots can achieve high dynamic gait with their torso soaring like quadruped mammals in nature, such as gallop, flying trot, and bound. In this paper, the focus is on the quadruped robot flying trot motion to achieve the stable and robust high dynamic motion of the robot.

A flying trot is a special kind of trot pattern characterized by a ballistic torso motion, in which one diagonal leg pair moves simultaneously, alternating with the other pair of legs and by a period in which there are no legs in contact with the ground. Few quadruped robots can achieve this kind of dynamic gait, which is summarized as follows. Through good mechanism design, the Cheetah-cub robot achieves fast motion of 6.9 times the robot length per second based on an open loop control method [4]. The results are limited to small dimensional designs. Due to the stable behaviour of the compact, small and lightweight quadruped robot itself, the control method of Cheetah-cub is hard to be transferred to the large robots with load capacity. The HyQ robot first realized the flying trot motion based on the active compliance control method [5]. The method is based on well-adjusted parameters that match the resonant frequency determined by the mass and the stiffness of the leg in the robot stance phase. Based on an online ZMP motion planner and continuously updates the reference motion trajectory as a function of the contact schedule, the ANYmal robot, developed at the ETH Zurich, can execute dynamic gaits including flying trot, jump, pronk and others [6]. By simplifying the dynamics model, MIT Cheetah 3 and Mini-Cheetah [7] convert the motion control problem into a convex optimization problem of ground reaction force based on model predictive control (MPC). According to this, the stand, trot, flying trot, pronk, bound, pace and other gaits movements are achieved. All of the above implementation methods have high requirements on the robot structural design and dynamics model, and the robots are all small and light-weight, lower than 100 kg. For quadruped robots with large size and mass, the flying trot is rarely studied.

The above methods are all based on robot model control. Methods based on reinforcement learning have become a hot spot in recent years. Tan et al.[8] add constraints such as hardware delay and controller output saturation to the training model on Minitaurs robot using deep reinforcement learning, which solves the gap between simulation and actual robot applications. ANYmal achieves an unconventional gait by deep reinforcement learning, which is between trot and flying trot, and greatly improves speed and robustness compared with the manual designed gait [9]. Peng et al. make the robot learn agile motion by reinforcement learning through example guided method [10], [11]. Although some groups have applied these simulation methods based on reinforcement learning to the actual platform, failures in the previous motion data acquisition and application cause huge costs to the robot prototypes, especially for large robots, a single failure in the training process may cause irreparable consequences for the robot.

The main contribution of this paper is a complete control method for the quadruped robot to achieve stable flying trot gait. In detail, the advantages of the method can be summarized as follows. The control framework consists of motion planning and terrain adaptation, which is modular and easy to embed in different platforms. The method proposed in this paper is robust for the robot to resist a certain range of external forces and climb 20° slope under flying trot gait

*This work was supported in part by the National Natural Science Foundation of China [Grant No. U1613223, 61973191], and in part by the National High Technology Research and Development Program of China [Grant No. 2015AA042201].

[1]Authors are with the Center for Robotics, School of Control Science and Engineering, Shandong University, China, corresponding author: Lelai Zhou email: zhoulelai@sdu.edu.cn

978-1-7281-6321-5/19//$31.00 ©2019 IEEE

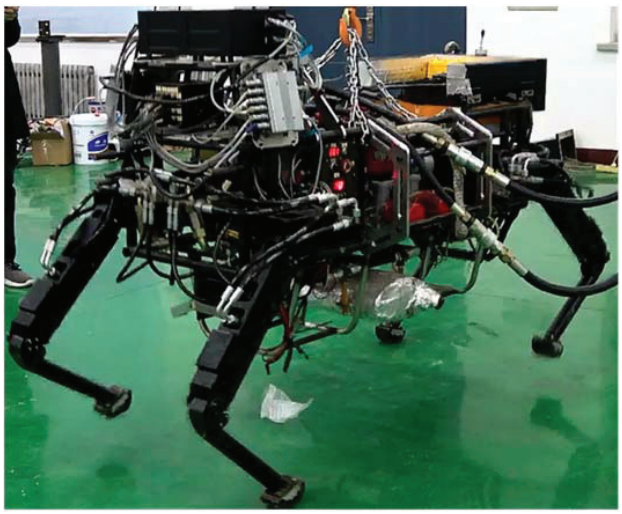

Fig. 1. The quadruped robot SCalf-III

in simulation. Few open method for the quadruped robot can achieve lateral impact recovery and climb slopes using the flying trot gait, which is the highlight of this work.

This paper is organized as follows. Section II describes the platform of the quadruped robot SCalf-III. The flying trot planning method is presented in Section III. Section IV introduces the strategies for slope adaptation and gaits transition. Section V contains simulation and implementation details and results.

II. Platform of the Quadruped Robot

SCalf-III [12] is a hydraulic actuated quadruped robot, developed by Shandong University as shown in Fig. 1. Each leg consists of 3 rotating joints that are the roll joint used to adduction and abduction at the hip, the pitch joint used to flexion and extension at hip and the pitch joint used to flexion and extension at the knee. Each joint is actuated by a hydraulic cylinder which is controlled by a servo value with position and force sensors.

The main control system is a set of NI controller Raco-9063 running on a Unix-like real-time operating system. The analogy signals about position and force sensors are collected by a 16-bit module NI 9220 at 1 kHz. Valves are controlled by a 16-bit analog output module NI 9264 with self-designed voltage controlled current circuit. The attitude angle and angular velocity of the robot torso are measured by VG440 at 100 Hz. The robot controller and remote controller are connected via radio station to send and receive control instructions at 30 Hz.

III. Flying Trot Controller

This section introduces the motion planning of the robot, which is divided into vertical direction planning and horizontal planning. They are used to achieve flying motion and balance control.

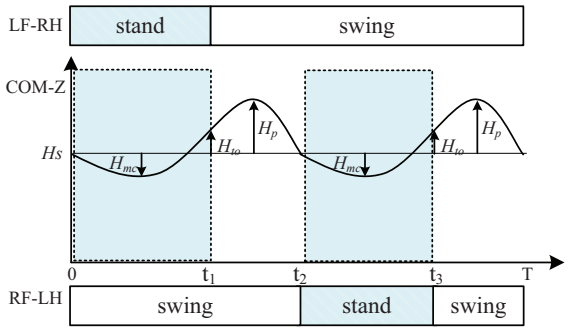

(a) Torso trajectory of the quadruped with flying trot gait.

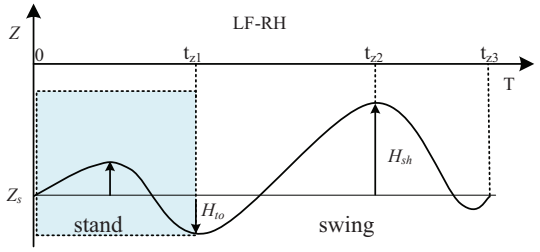

(b) Leg trajectory along Z axis

Fig. 2. Flying trot gait trajectory.

A. Vertical Direction Planning of Flying Trot Gait

A motion cycle of the flying trot gait consists of a support movement and a swing movement of the diagonal legs. The trend of the torso movement is shown in Fig. 2(a), and the movement of the diagonal legs in one cycle is shown in Fig. 2(b). In order to realize this kind of motion, the following motion law can be obtained based on kinetic energy and potential energy conversion in the sagittal plane.

$$\begin{aligned} t_{air} &= -\sqrt{2g(H_{to}-H_p)}/g + \sqrt{-2H_p/g} \\ t_{stand} &= (1/f - 2t_{air})/2 \\ t_{swing} &= \frac{1}{2}f + t_{air} \\ v_{to}^B &= -\sqrt{2g(H_{to}-H_p)} \\ v_{td}^B &= v_{to}^B + gt_{air} \end{aligned} \tag{1}$$

where H_s is the torso height when the robot is standing normally, H_{mc} indicates the offset of the lowest point of the torso movement, H_{to} stands for the offset of the torso height when the robot feet leave the ground, H_p is the highest torso offset during a flying trot period. t_{air} is the robot vacant time, when all the legs are in the air, t_{stand} and t_{swing} are the support phase and swing phase time, respectively. v_{to}^B and v_{td}^B are the speed of the torso along the z-axis when the leg phase of the robot changes from the support to the swing and from the swing to the support. g is the gravitational acceleration, and we set it to $-9.8\ m/s^2$.

The motion of the torso is mapped to the leg motion, which is decomposed into the following three parts. (a) The leg is

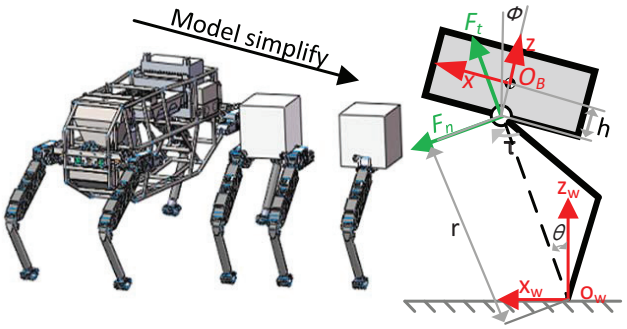

Fig. 3. Simplified model

buffered to reduce the impact force, which is realized by designing the speed as $v_{td}^{B}\lambda_0$ (λ_0 is minus) at time t_0. After reaching the maximum compression H_{mc}, the leg elongation begins. At the time of t_{z1} the leg begins to leave the ground. At this moment, the amount of leg extension and the variation of the torso position from the normal standing are same as H_{to}. (b) The leg enters the swing phase, and the leg is lifted to the target height at t_{z2}, when the vertical speed is 0. (c) Swing leg drop stage, during which time the leg recovers the normal standing height and wait to become the support leg. The summary of the leg position and speed at the key time points are shown in the Tab. I.

TABLE I

POSITION AND SPEED PARAMETERS OF THE LEGS AT KEY POINTS

Time	Position	Speed
t_0	Z_s	$v_{td}^{B}\lambda_0$
t_1	$Z_s - H_{to}$	0.2
t_2	$Z_s + H_{sh}$	0
t_3	Z_s	$v_{td}^{B}\lambda_0$

In implementation, a cubic interpolation curve is used to connect the constraint points composed of key position and speed to achieve smooth motion. Our previous work [13] has a more detailed description of this.

B. Horizontal direction planning of Flying trot

In order to maintain the stability of the robot torso during the movement, the quadruped model is simplified as an equivalent biped and then a single-leg jump model [14] for dynamic analysis as shown in Fig. 3. The simplified dynamic model is expressed as follows.

$$\begin{aligned} m(\ddot{x} - \ddot{\phi}h) &= -F_t sin(\theta) - F_n cos(\theta) \\ m(\ddot{z} - \dot{\phi}^2 h) &= F_t cos(\theta) - F_n sin(\theta) - mg \\ I\ddot{\theta} &= \tau - F_t hsin(\theta) - F_n hcos(\theta) \end{aligned} \tag{2}$$

where F_t and F_n are the forces exerted by the leg on the hip joint along the direction of the simplified straight leg and the vertical direction of the leg respectively. x and z are the torso center position on world coordinate $\{O_w\}$, m is the robot mass and h is the distance between the hip joint and the torso center. I is the robot moment of inertia moment. By eliminating F_t and F_n, acceleration of the torso pitch can be written as

$$\ddot{\phi} = \frac{\ddot{x}m(h+z) + xm(g - h\dot{\phi}^2 + \ddot{z})}{I + mh^2 + zmh} \tag{3}$$

By integrating, $\dot{\phi}$ is obtained

$$\begin{aligned} &\dot{\phi} = \frac{(\dot{x} - \dot{x}_0)m(h+z) + \int xm(g - h\dot{\phi}^2)dt}{I + mh^2 + zmh} = A\dot{x} + B \\ &where \\ &A = \frac{m(h+z)}{I + mh^2 + zmh} \\ &B = \frac{\int xm(g - h\dot{\phi}^2)dt - \dot{x}_0 m(h+z)}{I + mh^2 + zmh} \end{aligned} \tag{4}$$

It can be seen that A is positive and the torso stability can be ensured when $(\phi - \phi_d)\dot{x} < 0$ and $|\dot{x}| > |B/A|$. Because B is difficult to calculate, the constrain condition is simplified to $|\dot{x}| > k$, k is a number need to be tune. The trajectory in the support state is designed as follows

$$x(t) = x_0 - \int_0^t \dot{x}_d + k_p(\phi - \phi_d) - k_d(\dot{\phi} - \dot{\phi}_d)dt \tag{5}$$

where k_p and k_d are stiffness and damping parameters to balance the torso attitude, $\dot{x}_d$ is the desired robot velocity and x_0 is the initial position along x axis.

The swing state trajectory is designed based on SLIP model. The desired touch down position is

$$x_{fT} = \frac{\dot{x}T_s}{2} + k_{\dot{x}}(\dot{x} - \dot{x}_d) + x_0 \tag{6}$$

where the first term is used to maintain the desired velocity, and the second term is the compensation to the velocity error.

Analysis and design process in the y direction follow the same principle, which will no longer describe here.

IV. COMPLEX TERRAIN ADAPTATION STRATEGY

This section introduces the strategies to improve the stability and robustness of the quadruped robot, such as the slope adaptation strategy and gaits transition.

A. Slope Terrain Adaptation

To improve the stability and movement of the quadruped robot under the slope terrain, a mutually decoupled ground and torso adaptation strategy is proposed in this work. As shown in Fig. 4, the adaptation strategy consists of ground adaptation and torso adaptation.

To specify the adaptation method some coordinates and rotation matrix are needed. $\{W\}$ is the world coordinate. $\{B\}$ is the robot body coordinate, which is fixed at the center of the robot torso. $\{M\}$ is the foot position planning coordinate, which is used to connect the whole foot position adjustment process. $\{S\}$ is the slope topographic coordinate, and the origin is the intersection of the $\{M\}$ coordinate along the z axis and the slope.

When the pitch angle θ_{p_gnd} and roll angle θ_{r_gnd} of the terrain are known, the following relationship can be calculated.

$$^{M}_{S}\boldsymbol{R} = \boldsymbol{R}_y(\theta_{p\_gnd})\boldsymbol{R}_x(\theta_{r\_gnd}) \tag{7}$$

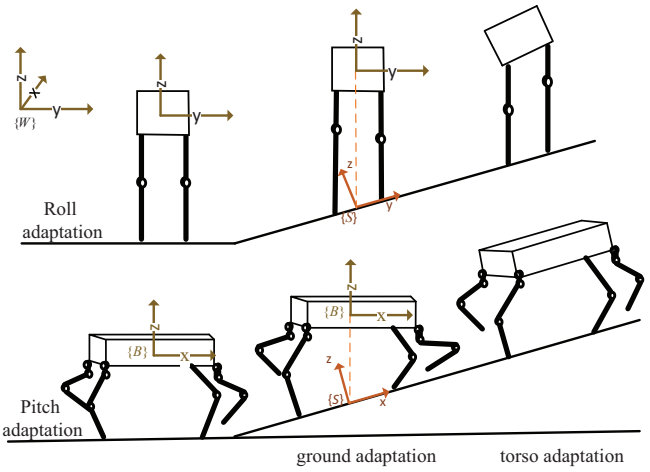

Fig. 4. Terrain-Adaptation

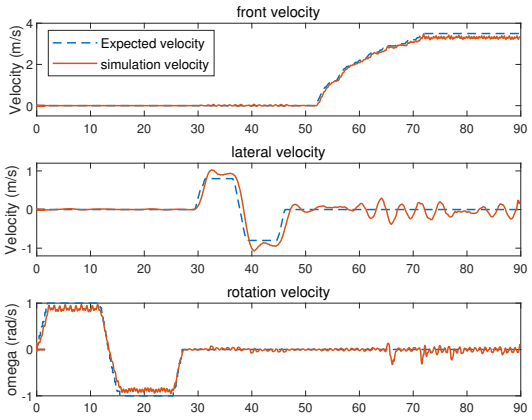

Fig. 5. Flying trot gait motion along x,y and z axis

The ground adaptation of the support leg is expressed as

$$\begin{aligned} {}^{M}\boldsymbol{P}_{toe} &= {}^{M}_{S}\boldsymbol{R}\,{}^{S}\boldsymbol{P}_{toe} + {}^{M}\boldsymbol{P}_{S0} \\ &= \boldsymbol{R}_y(\theta_{p\_gnd})\boldsymbol{R}_x(\theta_{r\_gnd})\,{}^{S}\boldsymbol{P}_{toe} + {}^{M}\boldsymbol{P}_{S0} \end{aligned} \tag{8}$$

where ${}^{S}\boldsymbol{P}_{toe}$ is the foot position in the $\{S\}$ coordinate, ${}^{M}\boldsymbol{P}_{S0}$ is the origin of the coordinate $\{S\}$ in the $\{M\}$ coordinate, which is $[0,0,-H]^T$. Assume that the pitch and roll angles of the torso adjustment are φ_{p_body} and φ_{r_body}, respectively.

$${}^{M}_{B}\boldsymbol{R} = \boldsymbol{R}_z(\varphi_{y\_body})\boldsymbol{R}_y(\varphi_{p\_body})\boldsymbol{R}_x(\varphi_{r\_body}) \tag{9}$$

Because the $\{M\}$ coordinate and the $\{B\}$ coordinate are both fixed at the centroid of the robot torso so ${}^{B}\boldsymbol{P}_{M0} = \boldsymbol{0}$. Considering the nature of the basic rotation matrix $\boldsymbol{R}_n^{-1} = \boldsymbol{R}_n^T$, the torso adaptation can be written as follows

$$\begin{aligned} {}^{B}\boldsymbol{P}_{toe} &= {}^{B}_{M}\boldsymbol{R}\,{}^{M}\boldsymbol{P}_{toe} + {}^{B}\boldsymbol{P}_{M0} \\ &= \boldsymbol{R}_x^T(\varphi_{r\_body})\boldsymbol{R}_y^T(\varphi_{p\_body})\boldsymbol{R}_z^T(\varphi_{y\_body})\,{}^{M}\boldsymbol{P}_{toe} \end{aligned} \tag{10}$$

The torso posture of the robot is measured by the body IMU. When the torso posture and the terrain posture of the robot are consistent, $\phi_{p\_imu} = \theta_{p\_gnd} = \varphi_{p\_body}$ and $\phi_{r\_imu} = \theta_{r\_gnd} = \varphi_{r\_body}$, the stability of the slope motion performance can be guaranteed. At this point, the robot leg and torso have the reasonable posture, then the ground adaptation and torso adaptation processes are simplified as:

$$\begin{aligned} {}^{B}\boldsymbol{P}_{toe} &= \boldsymbol{R}_x^T(\varphi_{r\_body})\boldsymbol{R}_y^T(\varphi_{p\_body})\boldsymbol{R}_z^T(\varphi_{y\_body})\,{}^{M}P_{toe} \\ &= \boldsymbol{R}_x^T(\phi_{r\_imu})\boldsymbol{R}_y^T(\phi_{p\_imu})(\boldsymbol{R}_y(\phi_{p\_imu}) \\ &\quad \boldsymbol{R}_x(\phi_{r\_imu})\,{}^{S}_{toe}\boldsymbol{P} + {}^{M}\boldsymbol{P}_{S0}) \\ &= {}^{S}_{toe}\boldsymbol{P} + \boldsymbol{R}_x^T(\phi_{r\_imu})\boldsymbol{R}_y^T(\phi_{p\_imu})\,{}^{M}\boldsymbol{P}_{S0} \end{aligned} \tag{11}$$

B. Gaits transition

Flying trot gait can achieve fast and efficient motion, but its stability is worse than trot gait. Stability in large external force disturbance and rugged terrain is hard to realize under flying trot gait of the quadruped robot. The purpose of the transition between the trot and flying trot is to improve the motion efficiency on flat terrain and adaptability on rugged terrain.

In this work, the gaits transition between trot and flying trot is not complicating. Setting the torso motion amplitude H_p and leg height variable H_{to} to 0 in motion designation, the trot gait can be achieved based on the proposed control framework.

V. Simulations and Experiments

In order to verify the control method proposed in this paper, a quadruped robot with the same size and inertia as the SCalf-III robot is built in dynamic simulation software Webots. The joint rotation limitation and output moment of the robot are constrained to be consistent with the actual platform. The flying trot gait motion and complex terrain adaptability of the quadruped robot are verified by simulation. The experiment of the flying trot gait is tested on robot physics platform. The important parameters for simulation and physical experiments are shown in Tab. II, and the results and explanations show in detail as follows.

TABLE II
Control Parameters

Variable	Simulation	SCalf-III
T_s	0.198 s	0.198 s
T_f	0.469 s	0.469 s
H_{sh}	250 mm	100 mm
k_{px}	40 mm/(rad.s)	40 mm/(rad.s)
k_{dy}	-0.01 mm/rad	-0.05 mm/rad
$k_{\dot{x}}$	0.2	0.15
$k_{\dot{y}}$	0.2	0.15

A. Simulations

1) Flying Trot Motion Test: In order to test the flying trot motion of the proposed method for quadruped robots, the forward-clockwise rotation command is first given as shown in Fig. 5. The robot can track the target rotation speed 1 rad/s in both sides. At time 30 s the lateral motion is tested, and finally the forward motion command is given. The robot

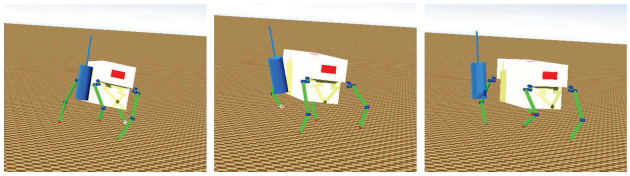

Fig. 6. lateral impact recovery

can stabilize the maximum forward speed at 3.5 m/s. Figure 5 shows that the proposed method can make the quadruped robot realize the three-dimensional motion under the flying trot gait .

2) Flying Trot Robustness: Robustness is demonstrated by the lateral impact recovery.

Due to the structural characteristics of the quadruped robot, the lateral stability is worse than the axial stability, which means that the lateral disturbance of the robot is more likely to destabilize the robot. Many quadruped robots can achieve stability after lateral impact using the trot gait [15], [16], [17], but few control algorithms can realize lateral impact recovery under flying trot gait. In the simulation, a 60 kg weight pendulum is placed 1.4 m above the ground, where the robot torso is 0.85 m. The pendulum can rotate freely to bump the robot. When the external forces drive the torso posture unstable, the legs in the supporting phase are adjusted based on Eq. (5). On the other hand, the disturbance causes the undesired motion of the robot, which is converges by the closed-loop correction of the swing phase based on Eq. (6), ensuring the stable motion of the robot.

The snapshots of the adjustment process after lateral impact are shown in Fig. 6. The torso attitude angle and adjustment speed during the adjustment process are shown in Fig. 7. At 3.2 s, the robot is tilted by a lateral angle of 12°, and the robot recover stable after about 2 s. It can be seen that the proposed control method has good robustness against external disturbances.

3) Slope Adaptation under Flying Trot Gait: In order to realise stable motion of the robot on the slope, the attitude control method designed in Eq. (5) are adjusted by making k_p and k_d zeros, The adaptation of the torso and the legs to the slope topography are based by the method detailed in section IV-A. As shown in Fig. 8, the robot can climb up and down the slope within 20° under flying trot gait. Based on the proposed control method, the robot can climb 30° slopes in trot gait because of the better stability than flying trot gait.

The motion of the quadruped robot using the flying trot gait on the slope terrain is the advantage of the proposed method. Many methods enable the quadruped robot locomote on slope under walk or trot gait[18], [19], [20]. Only the cheetah 3 robot achieves the flying trot motion on climbing up stairs[21]. In this paper, the proposed method make the quadruped robot climb up and down the slope terrain under the flying trot gait and all direction motion under the trot

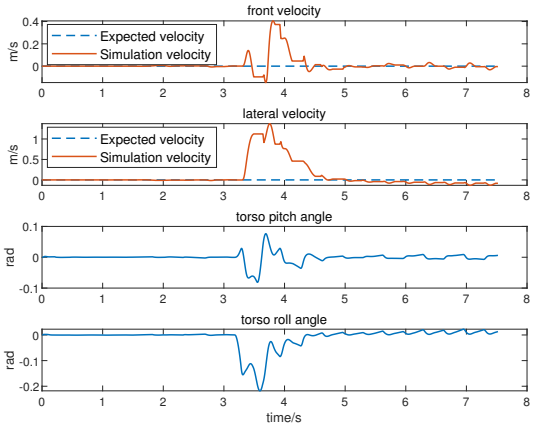

Fig. 7. Lateral impact recovery process

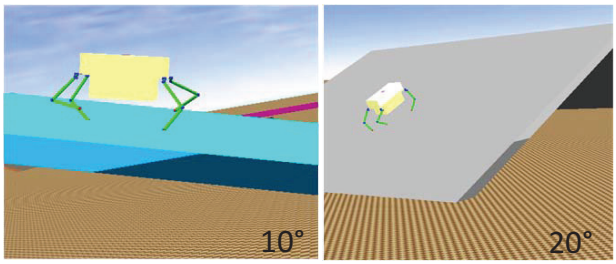

Fig. 8. Slopes Adaptation under flying trot gait

gait within 20°.

B. Experiments

The flying trot gait is tested on the SCalf-III prototype on flat terrain. For the sake of safety, the experiments on the slope are under the trot gait, which will not show in this paper. The result of the flying trot experiments are shown below.

The flying trot snapshots of SCalf-III are shown in Fig. 9. The leg motion and the touch force of the two front legs are shown in Fig. 10. The leg motion is calculated by the joint position sensor based on the leg kinematics, and the touch force is calculated by the joint force sensor and mapped to the foot force by the Jacobian matrix.

The interval between the two legs when the foot touch force is 0 indicates that none leg is in touch with ground in swing phase. The stable phase means that the robot can achieve stable flying trot motion.

VI. CONCLUSIONS

A flying trot control method for quadruped robots is proposed in this paper. By planning the robot torso movement and then mapping to the leg, the stable flying trot periodic motion is realized in the vertical direction. The dynamic balance problem based on the SLIP model is transformed into the problem of the foothold placement in the horizontal plane, which enables the robot to self-adjust

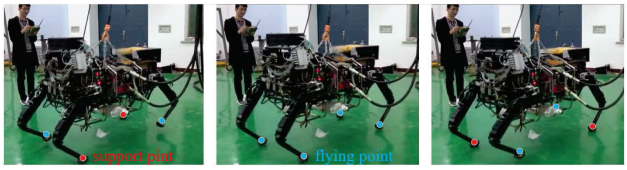

Fig. 9. Snapshots of flying trot in place on the SCalf-III robot

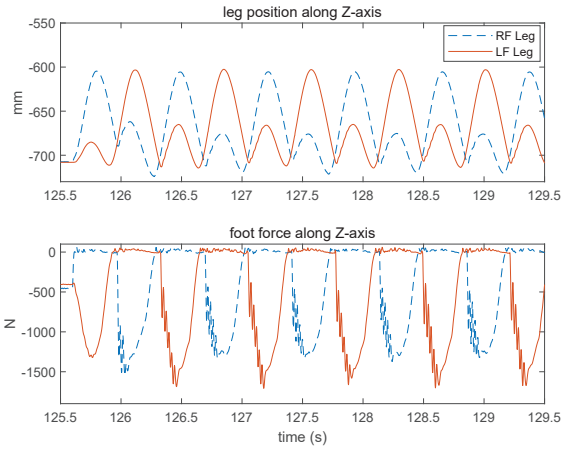

Fig. 10. Flying trot on the SCalf-III robot

and restore stability after being disturbed by external forces. In order to improve the motion ability under the slope terrain, a decoupled ground adaptation and torso adaptation strategy is proposed. Based on this control method, the up-and-down motion on slopes under flying trot gait is verified in simulation. Stable flying trot motion is verified on the physical platform Scalf-III robot.

REFERENCES

[1] B. Ugurlu, I. Havoutis, C. Semini *et al.*, "Dynamic trot-walking with the hydraulic quadruped robothyq: Analytical trajectory generation and active compliance control," in *2013 IEEE/RSJ International Conference on Intelligent Robots and Systems*. IEEE, 2013, pp. 6044–6051.

[2] C. Gehring, S. Coros, M. Hutler *et al.*, "Practice makes perfect: An optimization-based approach to controlling agile motions for a quadruped robot," *IEEE Robotics & Automation Magazine*, vol. 23, no. 1, pp. 34–43, 2016.

[3] T. Chen, X. Rong, Y. Li *et al.*, "A compliant control method for robust trot motion of hydraulic actuated quadruped robot," *International Journal of Advanced Robotic Systems*, vol. 15, no. 6, 2018.

[4] A. Spröwitz, A. Tuleu, M. Vespignani *et al.*, "Towards dynamic trot gait locomotion: Design, control, and experiments with cheetah-cub, a compliant quadruped robot," *The International Journal of Robotics Research*, vol. 32, no. 8, pp. 932–950, 2013.

[5] C. Semini, V. Barasuol, T. Boaventura *et al.*, "Towards versatile legged robots through active impedance control," *The International Journal of Robotics Research*, vol. 34, no. 7, pp. 1003–1020, 2015.

[6] C. D. Bellicoso, F. Jenelten, C. Gehring *et al.*, "Dynamic locomotion through online nonlinear motion optimization for quadrupedal robots," *IEEE Robotics and Automation Letters*, vol. 3, no. 3, pp. 2261–2268, 2018.

[7] J. Di Carlo, P. M. Wensing, B. Katz *et al.*, "Dynamic locomotion in the mit cheetah 3 through convex model-predictive control," in *2018 IEEE/RSJ International Conference on Intelligent Robots and Systems (IROS)*. IEEE, 2018, pp. 1–9.

[8] J. Tan, T. Zhang, E. Coumans *et al.*, "Sim-to-real: Learning agile locomotion for quadruped robots," *arXiv preprint arXiv:1804.10332*, 2018.

[9] J. Hwangbo, J. Lee, A. Dosovitskiy *et al.*, "Learning agile and dynamic motor skills for legged robots," *Science Robotics*, vol. 4, no. 26, p. eaau5872, 2019.

[10] X. B. Peng, P. Abbeel, S. Levine *et al.*, "Deepmimic: Example-guided deep reinforcement learning of physics-based character skills," *ACM Transactions on Graphics (TOG)*, vol. 37, no. 4, p. 143, 2018.

[11] X. B. Peng and M. van de Panne, "Learning locomotion skills using deeprl: Does the choice of action space matter?" in *Proceedings of the ACM SIGGRAPH/Eurographics Symposium on Computer Animation*. ACM, 2017, p. 12.

[12] K. Yang, L. Zhou, X. Rong *et al.*, "Onboard hydraulic system controller design for quadruped robot driven by gasoline engine," *Mechatronics*, vol. 52, pp. 36–48, 2018.

[13] T. Chen, X. Sun, Z. Xu *et al.*, "A trot and flying trot control method for quadruped robot based on optimal foot force distribution," *Journal of Bionic Engineering*, vol. 16, no. 4, pp. 621–632, 2019.

[14] M. H. Raibert, *Legged robots that balance*. MIT press, 1986.

[15] M. Raibert, K. Blankespoor, G. Nelson *et al.*, "Bigdog, the rough-terrain quadruped robot," *IFAC Proceedings Volumes*, vol. 41, no. 2, pp. 10 822–10 825, 2008.

[16] L. Lang, J. Wang, H. Ma *et al.*, "Compliant landing control of a trotting quadruped robot on unknown rough terrains," in *2015 IEEE International Conference on Information and Automation*. IEEE, 2015, pp. 1–6.

[17] Y. Shi, P. Wang, X. Wang *et al.*, "Bio-inspired equilibrium point control scheme for quadrupedal locomotion," *IEEE Transactions on Cognitive and Developmental Systems*, 2018.

[18] M. Focchi, A. Del Prete, I. Havoutis, and oters, "High-slope terrain locomotion for torque-controlled quadruped robots," *Autonomous Robots*, vol. 41, no. 1, pp. 259–272, 2017.

[19] S. Hirose, K. Yoneda, and H. Tsukagoshi, "Titan vii: Quadruped walking and manipulating robot on a steep slope," in *Proceedings of International Conference on Robotics and Automation*, vol. 1. IEEE, 1997, pp. 494–500.

[20] S. Fahmi, C. Mastalli, M. Focchi *et al.*, "Passive whole-body control for quadruped robots: Experimental validation over challenging terrain," *IEEE Robotics and Automation Letters*, vol. 4, no. 3, pp. 2553–2560, 2019.

[21] J. Di Carlo, P. M. Wensing, B. Katz *et al.*, "Dynamic locomotion in the mit cheetah 3 through convex model-predictive control," in *2018 IEEE/RSJ International Conference on Intelligent Robots and Systems (IROS)*. IEEE, 2018, pp. 1–9.